Effect of Sample and Substrate Electric Properties on the Electric Field Enhancement at the Apex of SPM Nanotips

ARTICLE *in* THE JOURNAL OF PHYSICAL CHEMISTRY B · SEPTEMBER 2005

Impact Factor: 3.3 · DOI: 10.1021/jp0523120 · Source: PubMed

2 AUTHORS, INCLUDING:

Alistair Elfick
The University of Edinburgh
86 PUBLICATIONS **898** CITATIONS

SEE PROFILE

ARTICLES

Effect of Sample and Substrate Electric Properties on the Electric Field Enhancement at the Apex of SPM Nanotips

Ioan Notingher† and Alistair Elfick*

University of Edinburgh, School of Engineering and Electronics, The King's Buildings, Edinburgh EH9 3JL, The United Kingdom

Received: May 4, 2005; In Final Form: June 27, 2005

Finite element (FE) models were built to define the optimal experimental conditions for tip-enhanced Raman spectroscopy (TERS) of thin samples. TERS experimental conditions were mimicked by including in the FE models dielectric or metallic substrates with thin dielectric samples and by considering the wavelength dependence of the dielectric properties for the metallic materials. Electromagnetic coupling between the substrate/sample and the SPM tips led to dramatic changes of both the spatial distribution and magnitude of the scattered electric field which depended on the substrate dielectric permittivity and excitation wavelength. Raman scattering as high as 10^8 with a spatial resolution of ∼8 nm was estimated for gold SPM tips and gold substrate when excitation is performed at 532 nm (near-resonance wavelength). For dielectric samples (∼4 nm thick), the enhancement of Raman scattering intensity is estimated at $\sim 10^5$; this does not depend significantly on the sample dielectric permittivity for dielectric samples. These results suggest that TERS experimental conditions should be estimated and optimized for every individual application considering the geometric factors and electric properties of the materials involved. Such optimizations could enlarge the range of applications for TERS to samples eliciting weaker intrinsic Raman scattering, such as biological samples.

Introduction

Recent developments in nanotechnology have led to an increased need for analytical tools able to provide topographical and physiochemical information about a sample with spatial resolutions in the 1−100 nm range. The highest spatial resolution of far-field optical instruments is diffraction limited to approximately 200 nm. While suitable for a large range of optical spectroscopy applications, a large numbers of samples and phenomena occur at lower scales (below 100 nm) and hence cannot be explored by far-field methods. Topographical information for a sample can be obtained with nanometric resolution using one of the scanning probe microscopy (SPM) methods (atomic force microscopy (AFM), scanning tunneling microscopy (STM), etc). Of particular interest are optical scanning probe techniques, as they may provide simultaneous spectroscopic information regarding atomic and molecular structure of the sample in a noninvasive fashion.[1]

Electromagnetic fields scattered by nanometric features of the sample are evanescent and therefore become attenuated within a few tens of nanometers from the sample surface.[1] To study these small features, either the excitation or detector has to be very close to the sample, i.e., in the near-field region. In scanning near-field optical microscopy (SNOM), the sample is irradiated through a subwavelength aperture (∼50 nm) at the end of a fiber probe maintained a few nanometers above the sample through a shear-force feedback mechanism.[2] This method provides simultaneous topographical and optical information about the sample with a resolution substantially below 100 nm. However, this method is ill-suited for spectroscopic measurement due to the low optical throughput of the aperture ($<10^{-4}$) and the large background originating from the Raman scattering and fluorescence in the fiber itself.

Tip-enhanced Raman spectroscopy (TERS) is based on the extremely high enhancement of the electric field observed at the apex of metallic SPM tips when excited with visible electromagnetic waves.[3] This method utilizes far-field illumination with the spatial resolution generally dictated by the size of the tip, which may be as small as 10 nm. The mechanisms of electric field enhancement (subsequently Raman scattering enhancement) are very similar to those observed in surface-enhanced Raman spectroscopy (SERS) where metallic substrates or colloids are used to enhance Raman scattering (see ref 4 for a review). Recent research[5] showed that SERS is able to study even single molecules, suggesting Raman scattering enhancements as large as $10^{14}-10^{15}$. Early theoretical studies[6] identified two main enhancement mechanisms to explain the strong Raman signal observed in SERS experiments: resonant excitation of surface plasmons in the substrate and the increase of the local field due to sharp edges and curvatures ("lightning rod effect"). These two enhancement mechanisms were shown to be strongly dependent on the shape, size, and dielectric properties of the metal objects. The wavelength dependence of the Raman scattering enhancement was attributed to the wavelength

* Corresponding author. E-mail: alistair.elfick@ed.ac.uk.
† E-mail: ioan.notingher@ed.ac.uk.

10.1021/jp0523120 CCC: $30.25
Published on Web 07/29/2005

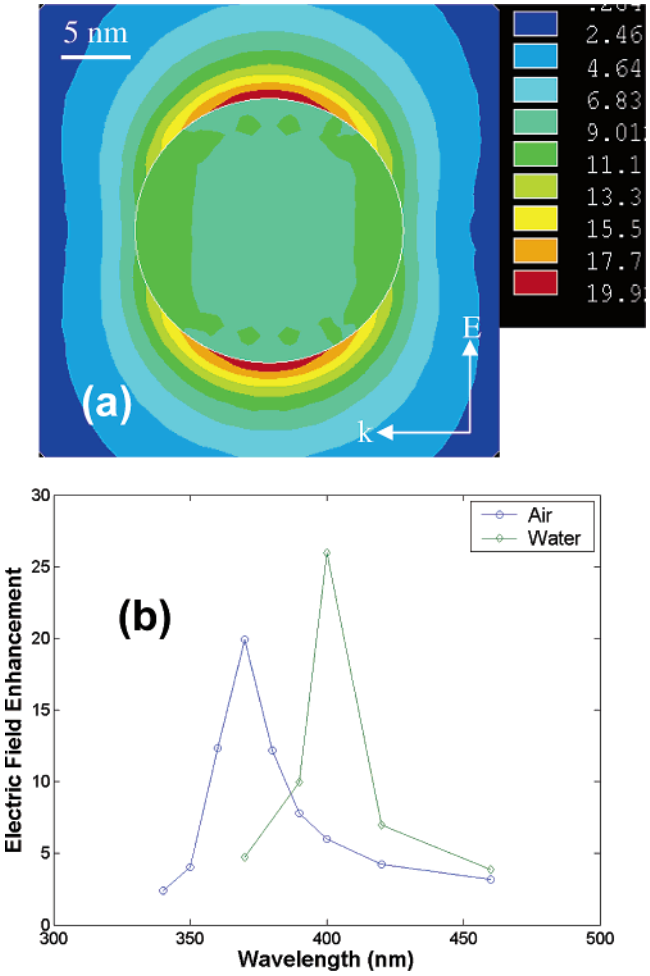

Figure 1. Electric field enhancement by a 20 nm radius Ag sphere: (a) distribution of the scattered electric field due to dipolar modes (370 nm laser); (b) maximum value of the scattered field as a function of laser wavelength in air and water.

dependence of the complex dielectric permittivity of the substrate which dictates the wavelength of the surface plasmon resonance. The lightning rod effect was perceived more as a geometric effect. However, recent studies have showed that, for nanoparticles, the geometry (size and shape) may also determine the surface plasmon resonance wavelength.[7,8]

There have been numerous studies on SERS during the past decades; however, experimental results using TERS are sparse. Recently, there have been several studies employing TERS using AFM tips,[9−11] shear-force microscopy,[12,13] and STM.[14] A poor understanding of the optimal conditions under which maximum enhancement may be obtained, especially for samples eliciting low Raman scattering (i.e., biological specimens), has contributed to the limited application range of TERS. Experimental optimization of TERS would require tunable lasers allowing measurements of the electric field enhancement for specific tip geometries, substrates, and samples over an extended excitation spectral region.

Theoretical computations are more easily implemented and represent a more feasible way to optimize the experimental conditions. However, the only analytically solvable problem for electromagnetic wave scattering by nanoparticles is given by Mie's theory and applies only to spheres.[15] The range of analytical solutions to other simple particle geometries may be extended by replacing Maxwell's equations with the Laplace equation (electrostatic approximation), but the solutions become

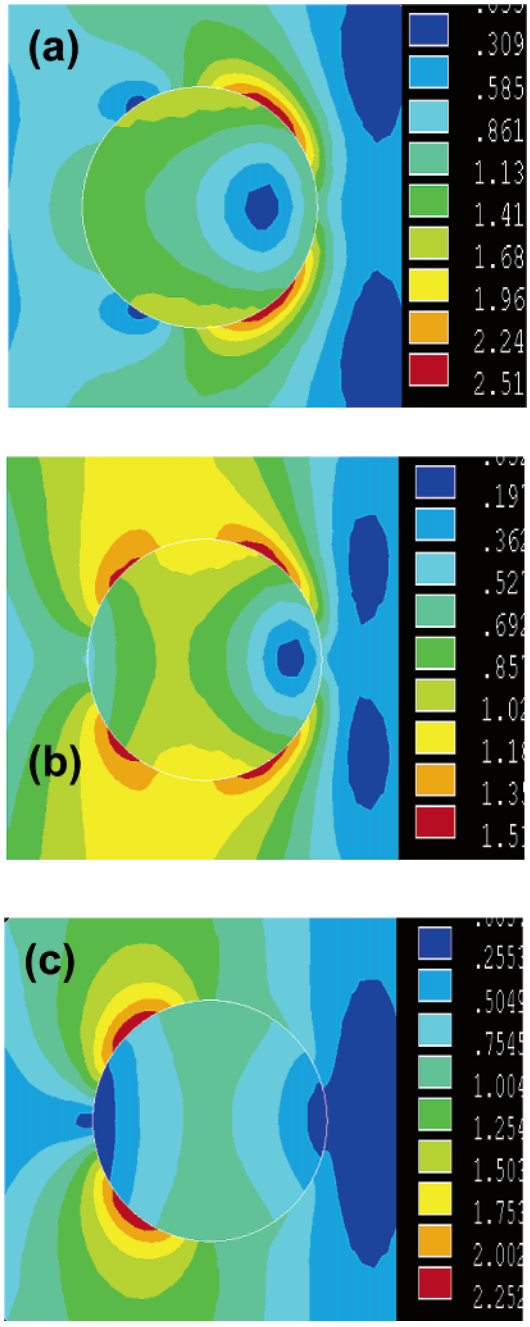

Figure 2. Excitation of multipole modes in 60 nm radius Ag spheres in air at various laser wavelengths: (a) 355 nm; (b) 358 nm; (c) 360 nm.

inaccurate for particle sizes larger than 10−20 nm as the field retardation effects become significant. Various computer simulation techniques have been applied to estimate the scattering of electromagnetic waves of regular[8,16−18] and even irregular particles.[19−21] Approximation methods, such as the multiple multipole (MMP) method,[22] the finite difference time domain,[23−25] and the finite element (FE) method,[26,27] were also applied to estimate the electric field enhancement and subsequently the enhancement of Raman scattering by the apex of metallic SPM tips.

The majority of studies to date are limited to the estimation of electric field enhancement around SPM tips in free space, conditions that are dissimilar to those encountered experimentally. In these simulations it was assumed that the presence of the sample and substrate do not influence the magnitude and

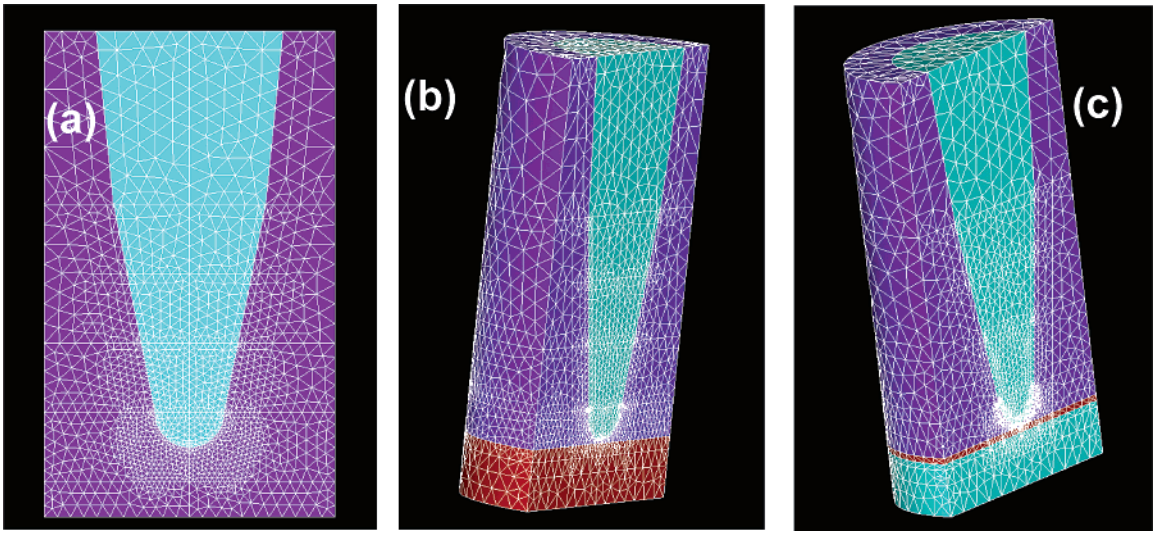

Figure 3. FE models of a 20 nm radius tip: (a) without substrate, 2D; (b) 2 nm above a substrate, 3D; (c) 2 nm above a 4 nm thick layer sample on a thick substrate, 3D.

spatial distribution of the scattered electric field, and therefore they were not included in the models. Moreover, the effect of excitation wavelength and wavelength-dependent dielectric properties for the excitation of surface plasmons resonances in the apex of the tip were not considered. Models including metallic tips above metallic substrates were solved using the Laplace method, but the effect of wavelength-dependent dielectric properties of the substrate or sample had not been analyzed.[21] Dielectric substrates and theoretical models of the dielectric permittivity of metal tips (Drude model) were introduced in FDTD simulations, showing the importance of resonant excitation on the maximum Raman scattering enhancement.[23,24]

The aim of the present study is to take the theoretical computations further by using an FE method to estimate the effect of the dielectric properties of the substrate and sample on the electric field enhancement by SPM tips. These conditions are more realistic, better mimicking the conditions encountered in experimental situations. We show that the presence of a sample and substrate influence directly the magnitude and spatial distribution of the electric field, and the selection of excitation wavelength is paramount for maximizing the Raman scattering enhancement.

Methods

FE models were built and used to determine the magnitude and spatial distribution of the electric field scattered by metallic objects with sizes smaller than 100 nm. In an FE electromagnetic problem, a geometric model is built and then divided into smaller domains (elements). Maxwell's equations are solved for each individual element after the application of the appropriate boundary conditions and loads; the solutions of the Maxwell's equations produce the magnitude of the electric field for each individual element of the model. In this study, we used the ANSYS Multiphysics software for high-frequency electromagnetic simulations in the frequency domain (Ansys Inc., U.S.A.).

The nanoscopic objects modeled were metallic spheres and sharp tips, similar in size to the tips employed in SPM. Models of silver spheres (20 nm and 60 nm radii) and tips of gold and silver (20 nm apex radius, 10° divergence) were built as 3D volumes using first-order tangential vector tetrahedral elements. The number of elements for each model was about 50 000 (~75 000 nodes) and was chosen as a compromise between accuracy and computation time. The metallic materials used in our analysis were modeled as lossy dielectric materials, and their complex dielectric permittivity were obtained from experimental data available in the literature.[28] Each part of the model was meshed automatically; the size of the mesh was selected according to the relevance to the problem of each specific region. Regions of interest, i.e., around the tip apex, were divided into elements as small as 0.8 nm, while the elements in the parts of the model of less interest had sizes up to 15 nm (~30 times less than the wavelength of the excitation laser). Free space was modeled using the surface impedance boundary condition $Z = (\mu_0/\epsilon_0)$, where μ_0 and ϵ_0 are the magnetic permeability and dielectric permittivity of vacuum. The laser excitation was applied as a plane wave for which the propagation direction, polarization, and wavelength were defined. For all models described in this study, the propagation of the laser was along the horizontal *OX* axis and the polarization was along the vertical *OZ* axis. The magnitude of the incident laser electric field was set to 1; therefore, the magnitude of the computed scattered electric field is numerically equivalent to the electric field enhancement. The plane *OXZ* was set as a symmetry plane in order to simplify the models and increase the computational efficiency. The convergence of the FE models was checked by modifying the number and size of the meshing until errors of less than 5% were observed (except where otherwise stated).

Results and Discussion

Validation of FE Methods. The first step in our study was to model scattering of electromagnetic waves with frequencies in the optical spectrum by small (radii smaller than 100 nm) metallic spheres for which the analytical solution can be obtained using Mie's scattering theory[15] and computer simulation[8] and experimental data are available[29−32] for comparison.

An incident electromagnetic field will induce coherent oscillations of free electrons in metallic spheres along the direction of the electric field called dipole plasmon resonance. The frequency of the dipole plasmon resonance depends on the electric properties of the material and the size of the sphere. If the metal sphere is small, the dipole mode is the only electronic oscillation induced in the sphere (the sphere is uniformly polarized), and the solutions of the Maxwell's equations show that the distribution of the scattered electric field resembles the electric field produced by a radiating electric dipole. The

polarizability of the dipole depends on the size and dielectric permittivity (ϵ) of the sphere and shows a resonance peak for the excitation wavelength when the condition $\mathrm{Re}(\epsilon) = -2\epsilon_m$ is satisfied, where ϵ_m is the relative permittivity of the surrounding medium.[33] The excitation of the dipole plasmon resonance in a 20 nm radius silver sphere using our FE model is shown in Figure 1a (the propagation vector k and electric field intensity E_0 of the incident wave are shown on the figure by arrows). The wavelength dependence of the scattered electric field magnitudes when the silver sphere is in air and in water are shown in Figure 1b. In air, the maximum magnitude of the scattered electric field is ~20 times higher than the incident field when the excitation wavelength is 370 nm; this wavelength corresponds to $\mathrm{Re}(\epsilon) = -2.6 \cong -2$. When the sphere is in water ($\epsilon_{water} = 1.77$), a red-shift of the plasmon resonance peak to ~400 nm is observed, which corresponds to $\mathrm{Re}(\epsilon) = -3.774 \cong -2 \times 1.77$, as predicted by theory[33] and supported by experimental results.[29−32] When the size of the sphere is larger, the excitation field tends not to homogeneously polarize the particles, and higher order (multipole) surface plasmons are generated. The solutions of the Maxwell's equations show that higher multipole oscillations, such as the quadrupole mode, can also be excited and overlap on the lower modes leading to more complex electric field distribution within and around the spheres.[33] Figure 2 presents the scattered electric field by a 60 nm radius silver sphere for three excitation wavelengths indicating the excitation of quadrupole modes.

The FE simulation results are in good agreement with both published results obtained using other simulation techniques and experimental studies. Confirmation that the nanosphere models provide robust and accurate results thereby endorses the suitability of the FE models for the study of nanoscopic objects of interest that are less well characterized and for which experimental data are difficult to obtain.

Electric Field Enhancement by Sharp Metallic SPM Tips. *Model 1: SPM Tip in Free Space*. 2D and 3D images of the FE models for silver and gold tips with apex radii of 20 nm are shown in Figure 3. The geometry of the tips was chosen to represent that which may be manufactured feasibly. Recent published papers reported on the manufacture of silver and gold tips with radii of ~20 nm by electrochemical etching with supplemental focused ion beam milling.[12,34,35] Similar gold tips have been also obtained recently in our laboratory (data not shown).

The near-field distribution of the scattered electric field by a gold tip is shown in Figure 4a for the case where the excitation electromagnetic wave is linearly polarized along the vertical axis of the tip (*OZ* axis) and the propagation is along the horizontal axis (*OX* axis, in the plane of the figure) (wavelength 632 nm). The simulated spatial distribution and magnitude of the scattered field (10-fold enhancement) is in good agreement with published results using other computation techniques such as the multiple multimode model,[22] finite difference time domain,[23,25] frequency domain, and time domain FE.[26,27] Our simulations for other polarization directions (not shown), particularly along the *OX* axis, also agree with the literature and indicate an approximately 2-fold enhancement of the electric field. Since the enhancement of the axial component (~10) of the incident electromagnetic wave is much stronger, our study focuses on the case of lateral illumination with a vertical polarized monochromatic wave. Although the lateral illumination seems unfeasible, it has been shown recently that it can be achieved in modern instruments by using obliquely mounted microscope objectives.[14] Alternatively, on-axis illumination can be used to obtain vertical polarization if the tip is illuminated with one of the longitudinal field lobes obtained by tight focusing of a Gaussian laser.[12,36]

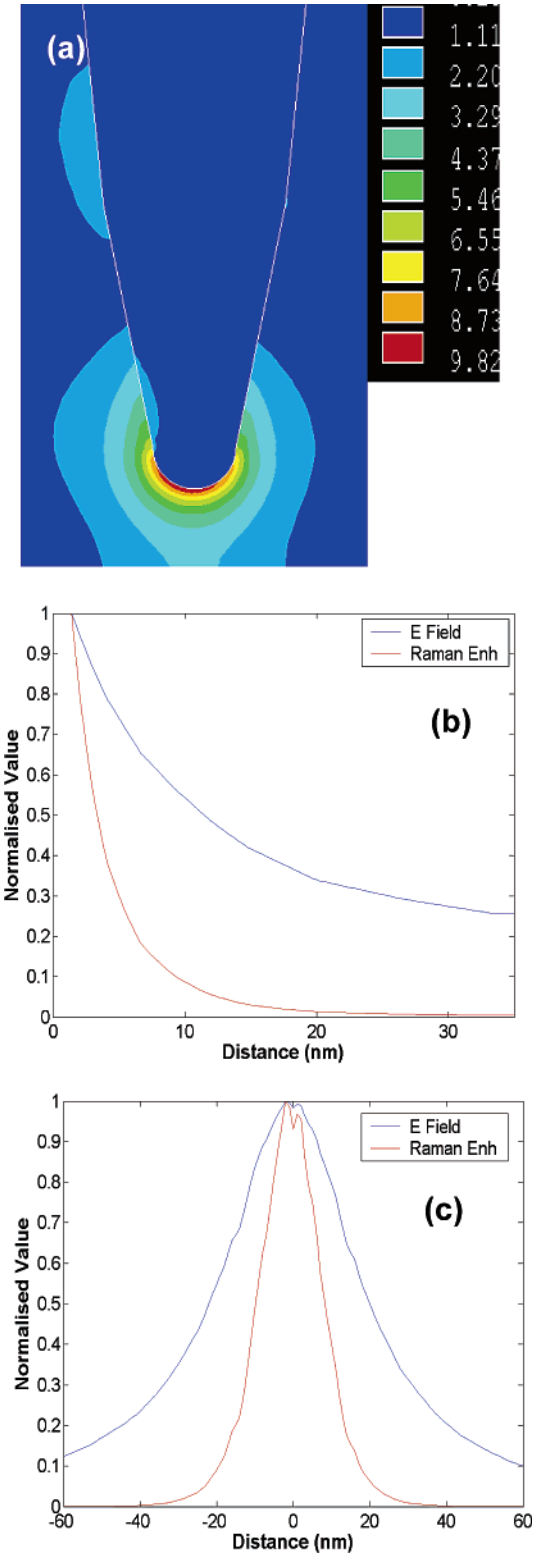

Figure 4. Distribution of the scattered electric field around a 20 nm radius gold tip in air: (a) FE map; (b) normalized electric field intensity as function of distance away from the tip along the vertical axis (*OZ*); (c) normalized electric field intensity along a horizontal line 2 nm below the apex of the tip (laser wavelength 632 nm). Note: Figure 4a, Figure 5, parts a and c, and Figure 7 all possess the same spatial scale.

The spatial distribution of the scattered electric field along the vertical axis, *OZ*, and horizontal axis, *OX*, are presented in

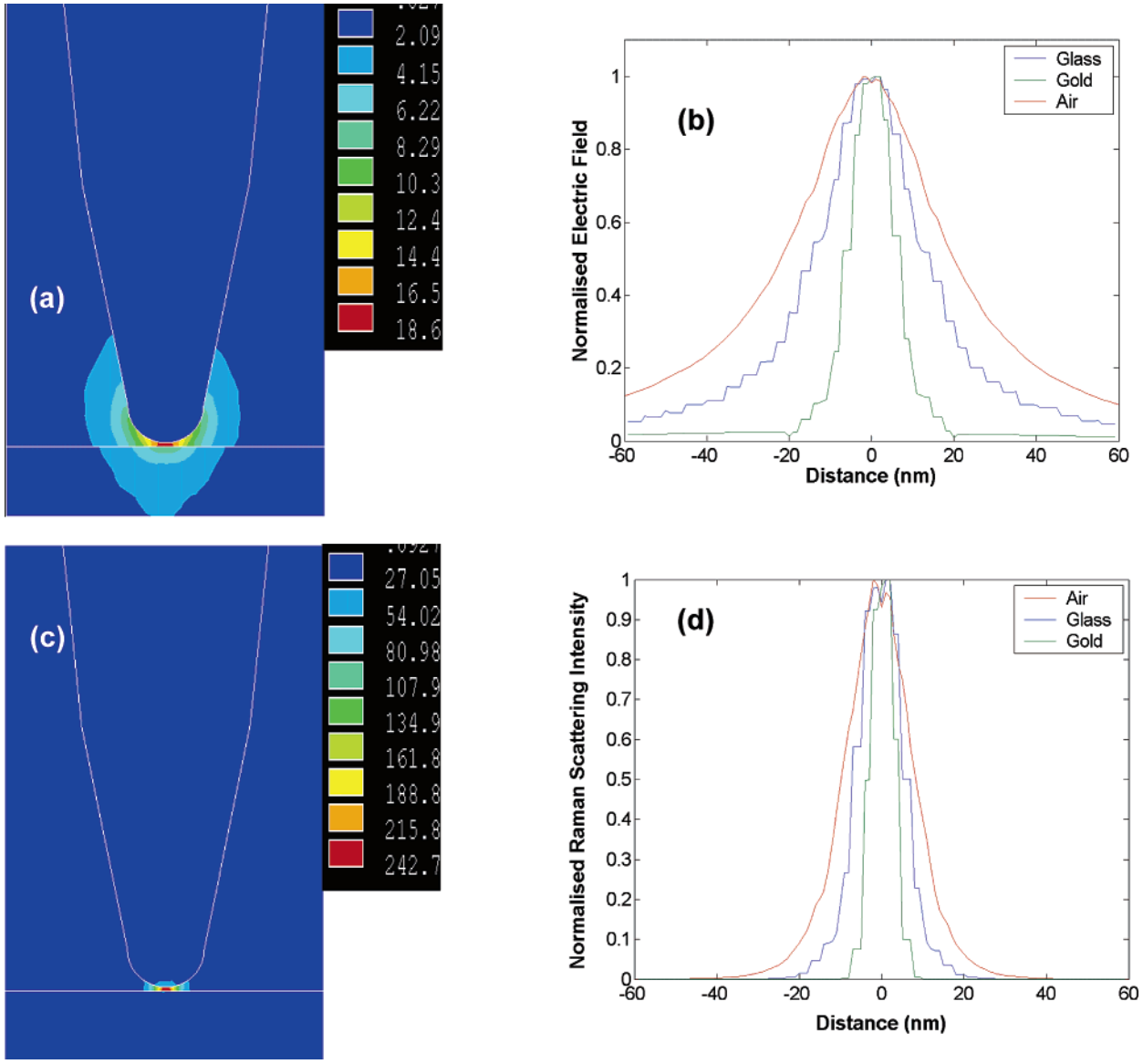

Figure 5. Electric field enhancement for 20 nm radius Au tips 2 nm above a substrate: (a) glass substrate, laser 660 nm; (b) normalized magnitude of the electric field in the lateral direction at a distance of 1.8 nm below the tip for all substrates; (c) gold substrates (laser 529 nm); (d) normalized magnitude of the Raman scattering in the lateral direction at a distance of 1.8 nm below the tip for all substrates.

Figure 4, parts b and c, respectively. The rapid decay of the electric field with distance away from the tip suggests that the sample must be placed very close to the tip in order to benefit from the high enhancement. Attention should be drawn to the fact that the measured signal in Raman spectroscopy is approximately proportional to the fourth power of the electric field; therefore, Raman scattering enhancement decays even faster with the increase of the tip−sample separation distance, suggesting a maximum tip−sample separation of ~5 nm (Figure 4b). The lateral distribution of the electric field affects directly the spatial resolution of a TERS measurement. Figure 4c shows that the lateral resolution for TERS imaging is approximately half the size of the tip (fwhh = 18.5 nm), i.e., it is no longer constrained by optical considerations.

Model 2: SPM Tip Above a Substrate. When a metal nanoparticle is placed in the vicinity of a substrate, its surface plasmon resonance changes due to electromagnetic coupling between the particle charges and the induced charges in the substrate.[37] The presence of the substrate influences both the frequency of, the width of, and may even split the single-particle plasmon resonance peaks.[37] A metallic substrate can have additional effects due to coupling of localized surface plasmons of the particle with the propagating surface plasmons at the substrate-free space interface.[38] Electromagnetic coupling of localized surface plasmons in nanoscale spheres separated by small distances showed surface plasmon spectra different to those corresponding to separated spheres,[8] with enhanced electric fields in the space between the spheres. Shifts of surface phonon resonances in dielectric nanospheres placed in the vicinity of dielectric and metallic substrates were also observed and reported to depend on the particle−substrate separation distance.[39] Therefore, for the estimation of optimal TERS experimental conditions, it is important to include a substrate in the FE models and to consider its dielectric properties. This model describes a more realistic experimental setup and provides insight into selecting the substrate material for optimal sample signal strength and spatial resolution.

In this work, the influence of the electric properties of a substrate on the enhancement and spatial distribution of the electric field was studied for three substrate materials: glass, gold, and silver. When a glass slab ($\mathrm{Re}(\epsilon) = 1.96$, $\mathrm{Im}(\epsilon) = 0$ for all wavelengths) was placed 2 nm below a gold tip (Figure

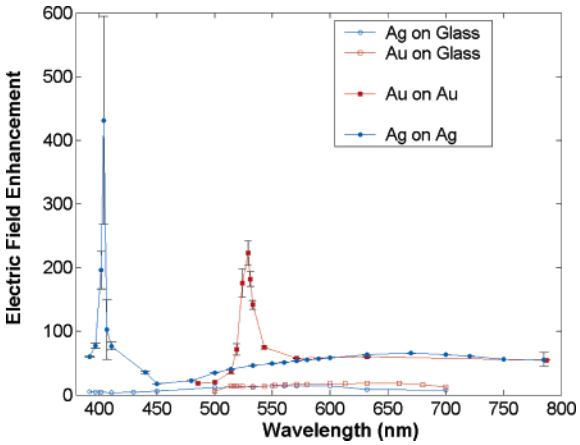

Figure 6. Dependence of the electric field enhancement on the laser excitation wavelength and substrate for 20 nm radius gold and silver tips.

5a), a maximum enhancement of the electric field of ~19 was obtained (excitation wavelength 660 nm), which represents a 2-fold increase compared to models that do not include a substrate. Figure 5a also shows that dielectric substrates tend to confine the electric field in the region between the tip and substrate. The distance dependence in the lateral direction (*OX*) of the electric field at the substrate surface is plotted in Figure 5b. The data suggest that the spatial resolution of TERS measurement in the horizontal plane *OXY* is improved to ~13 nm (fwhm).

Figure 5, parts c and d, presents the electric field distribution for gold SPM tips 2 nm above a gold substrate. The FE results indicate that the electric field is more strongly confined in the region between the tip and substrate and that the enhancement has increased dramatically to ~200, representing a 10-fold increase compared to the glass substrate case. This case also led to an increased spatial resolution of ~8 nm in the horizontal plane *OXY*. The values obtained in this more realistic case suggest that the spatial resolution is not limited solely by the tip geometry but can be increased by the right choice of substrate material.

Compared to the glass substrate case, a strong dependence of the electric field enhancement on the excitation wavelength was observed for metallic substrates (Figure 6), indicating the presence of a resonance effect. These resonances led to a dramatic increase of the electric field magnitude, by a factor of ~400 for a silver tip on silver substrate ($\epsilon = -3.99 + 0.681i$ at 404 nm excitation wavelength) and a factor of ~200 for a gold tip on gold substrate ($\epsilon = -5.335 + 2.276i$ at 529 nm excitation wavelength). The strong resonances led to variations in the FE-computed enhancement magnitudes compared to off-resonance wavelengths. The error bars plotted in Figure 6 were obtained by performing FE simulations on three similar models but with different mesh sizes and densities. While the errors at off-resonance wavelengths were ~1%, errors as large as 30% were observed for silver at 404 nm. These results suggest that the absolute values of the enhancement magnitude are less accurate but indicate reliably that a resonance phenomenon, probably due to electromagnetic coupling between SPM tips and metallic substrate, leads to a very large electric field enhancement at the tip apex. The electric field enhancements herein agree with those reported recently using FE computations for silver SPM tips (5 nm radius) close to 40 nm radius silver nanospheres.[26] The spatial distribution of the electric field was also similar to our results, showing strong confinement of the electric field in the region between the tip and substrate.

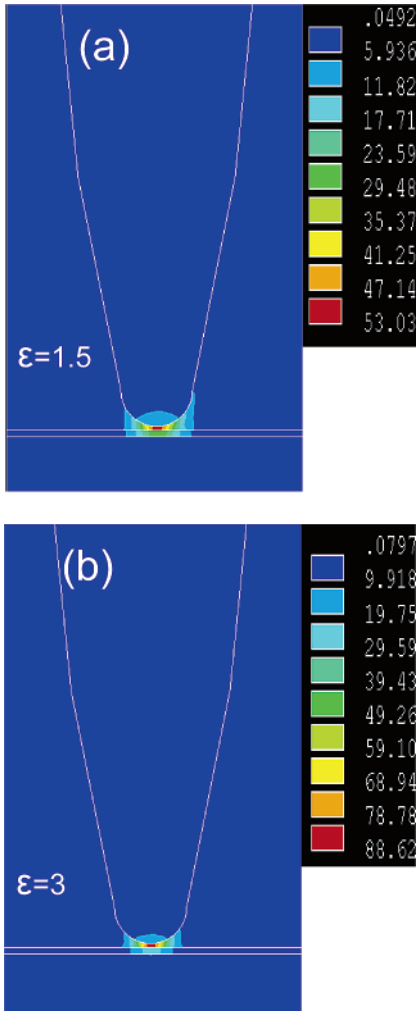

Figure 7. Electric field distribution when a 20 nm gold tip is brought 2 nm above a 4 nm thick layer sample on a gold substrate. Relative dielectric permittivity of the sample is as follows: (a) 1.5, 519 nm laser; (b) 3, 524 nm laser.

However, the authors performed the computations for a single wavelength (810 nm) and did not report a full enhancement spectrum. It is therefore difficult to judge whether their excitation was at resonance for their model.

Although the field enhancement for gold SPM tips was lower than for silver tips, the fact that the resonance occurs at 529 nm makes gold very attractive to experimentalists due to the availability of the Nd:YAG lasers for which the second harmonic occurs at 532 nm. This wavelength is slightly off resonance, but our FE models suggest enhancements of the electric field as high as ~150. When it is considered that the Raman scattering intensity is proportional to the product between the square of the excitation electric field ($E \sim 150$ at 532 nm) and the square of the emission electric field ($E \sim 90$ in the region of 536−634 nm corresponding to a 100−3000 cm^{-1} Raman shift), a Raman scattering enhancement of $\sim 10^8$ may be estimated when a gold substrate is used.

Model 3: SPM Tip above a Thin Sample Placed on Metallic Substrate. In view of the dramatic effect of excitation wavelength and substrate material, a realistic simulation of signal strength and spatial resolution in TERS experiments must include the sample. To consider this, the sample was defined as a 4 nm thin layer dielectric sample ($\mathrm{Re}(\epsilon) = 1$, 1.5, 2, and 3; $\mathrm{Im}(\epsilon) = 0$) on a bulk gold substrate. A 20 nm radius gold tip was place 2 nm above the sample (see Figure 3c).

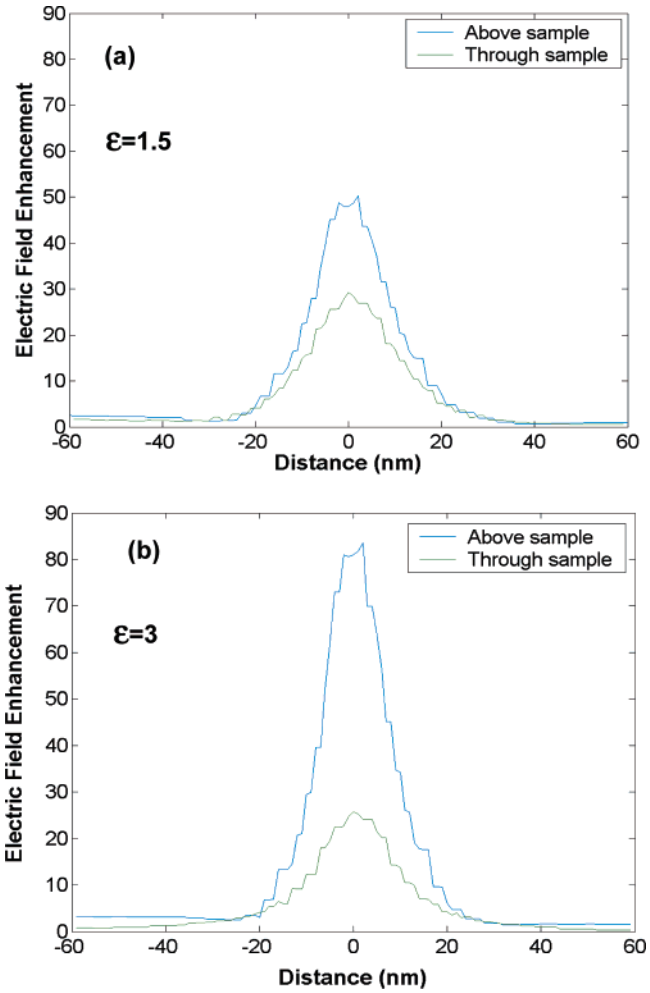

Figure 8. Magnitude of the electric field enhancement above and through the sample: (a) 1.5, 519 nm laser; (b) 3, 524 nm laser.

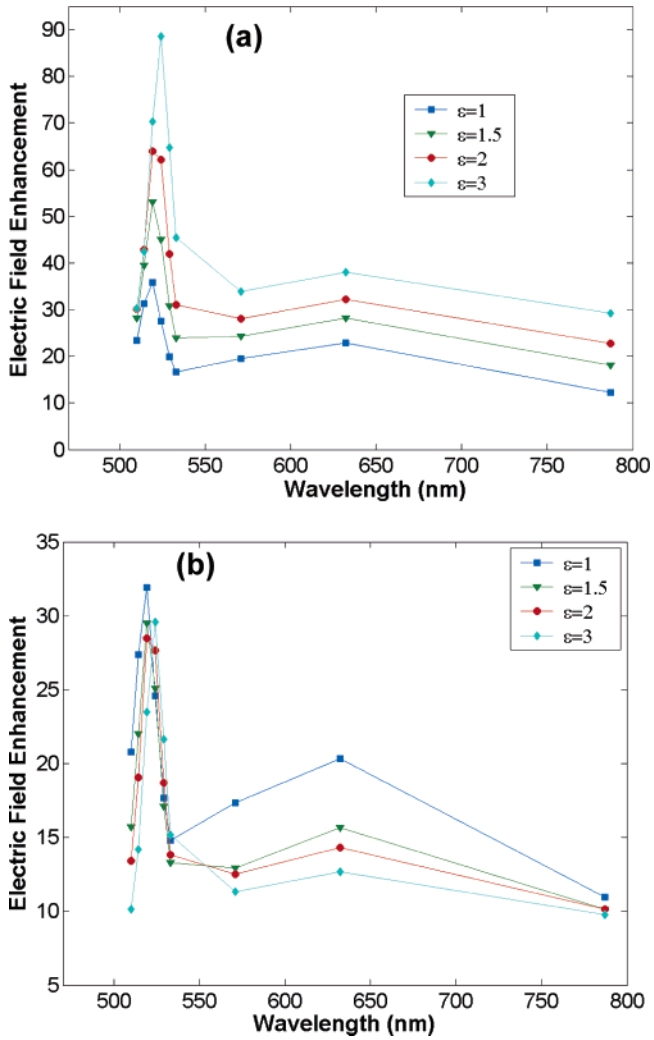

Figure 9. Electric field enhancement for 20 nm radius gold tips as function of the dielectric permittivity of the sample (4 nm thickness, 2 nm below the tip, on gold substrate): (a) above sample; (b) through sample.

The distributions of the electric field in the near-field region of the tip for two values of dielectric permittivity of the sample ($\mathrm{Re}(\epsilon) = 1.5$ and $\mathrm{Re}(\epsilon) = 3$) are shown in Figure 7. High enhancements of the electric field are observed between the tip and sample ($\sim$50 for $\mathrm{Re}(\epsilon) = 1.5$ and $\sim$90 for $\mathrm{Re}(\epsilon) = 3$); however, smaller enhancements were predicted within the thin sample. The electric field is slightly more confined for higher dielectric permittivity of the sample, though no significant improvement in spatial resolution was noticed as defined by the fwhm values (Figure 8).

The magnitude of the electric field has a significant dependence on the excitation wavelength, indicating the presence of a resonance peak, which shifts slightly ($\pm 2-3$ nm) depending on the sample dielectric permittivity (Figure 9). Although the field in the region between tip and sample is $\sim$2-fold higher for $\mathrm{Re}(\epsilon) = 3$ compared to $\mathrm{Re}(\epsilon) = 1.5$ (Figure 9a), the electric field within the sample varies insignificantly with the $\mathrm{Re}(\epsilon)$ of the sample around the resonance wavelength (Figure 9b). The spectral dependence of electric field enhancement allows an estimation of the Raman scattering intensity over a 3300 cm^{-1} Raman shift with excitation at 532 nm: excitation enhancement of $\sim$30, emission enhancement of $\sim$13, leading to a Raman scattering enhancement of $\sim 1.5\ 10^5$.

A comparison of the predicted Raman scattering enhancement obtained from our simulations with the experimental estimations reported in the recent literature lends credence to the approach presented. In a study of carbon nanotubes deposited on a glass substrate using a silver tip and laser excitation at 632 nm, a Raman scattering enhancement of $\sim 10^3$ was measured.[12] The FE simulations presented above predict that for a 20 nm Ag tip and a sample with $\mathrm{Re}(\epsilon) = 1.96$, the Raman scattering enhancement ($\sim 5 \times 10^3$) agrees well with Hartschuh et al.'s[12] value for the same excitation wavelength (632 nm) and Raman shift. A similar study of adsorbed molecules on gold substrates observed Raman scattering enhancements as high as 10^6 with laser excitation of 632 nm using gold tips of $\sim$40 nm radii.[14] The FE simulations herein suggest an enhancement of $\sim 2 \times 10^7$ for 20 nm radius gold tips on gold substrate. The higher value obtained from the FE computation may be accounted for by the smaller size of the tip used.

The use of FE models represents an efficient mechanism for the systematic investigation of electromagnetic parameters which influence TERS. Yet limitations exist pertaining to overlooked mechanisms, such as chemical enhancement, which has been observed experimentally in SERS measurements.[4] Notwithstanding this, the simulations presented offer a valuable insight into strategies for the sample-specific optimization of TERS. The experimental verification of the above work is underway.

Conclusions

Finite element (FE) models were built to estimate the optimal experimental conditions for tip-enhanced Raman spectroscopy

(TERS) of thin samples. First, the FE models of nanospheres were verified against simulation and experimental results available in the literature. Dipole and quadrupole plasmon resonances were observed for silver spheres and occurred at the wavelengths predicted theoretically and measured experimentally.

Realistic models of TERS experimental conditions were created by the inclusion of solid dielectric or metallic substrates and thin dielectric samples. Moreover, the material's wavelength-dependent dielectric properties were considered. Electromagnetic coupling between the substrate/sample and SPM tips led to dramatic changes of both the spatial distribution and magnitude of the scattered electric field which depended on the substrate dielectric permittivity and excitation wavelength. Emphasis was placed on gold tips and gold substrates due to the previously established methods to manufacture sharp SPM tips and smooth substrates. Raman scattering enhancements as high as 10^8 are estimated for gold SPM tips and samples adsorbed on gold substrates if excitation is performed near the resonance laser wavelength (532 nm). However, for thicker dielectric samples the enhancement of Raman scattering intensity is estimated at $\sim 10^5$ and does not depend significantly on the sample dielectric permittivity. At the same time, the gold substrate has a significant role on spatial resolution as it is improved to $\sim$8 nm, which is $\sim$5 times smaller than the tip.

The results presented suggest that experimental conditions should be estimated and optimized for every application considering the geometric factors and electric properties of the materials involved. Such optimizations could enlarge the range of application of TERS to samples eliciting weaker Raman scattering, including biological samples.

Acknowledgment. The authors thank the U.K. Engineering and Physical Sciences Research Council (EPSRC) for the financial support of this work (Grant No. GR/S52148/01).

References and Notes

(1) Fillard, J. P. *Near Field Optics and Nanoscopy*; World Scientific Publishing Co Pte Ltd: Singapore, 1996.
(2) Karrai, K.; Grober, R. D. *Ultramicroscopy* **1995**, *61*, 197.
(3) Wessel, J. *J. Opt. Soc. Am. B* **1985**, *2*, 1538.
(4) Moskovits, M. *Rev. Mod. Phys.* **1985**, *57*, 783.
(5) Nie, S.; Emory, S. R. *Science* **1997**, *271*, 1102.
(6) Gersten, J. *J. Chem. Phys.* **1980**, *73*, 3023.
(7) Jensen, T. R.; Malinsky, M. D.; Haynes, C. L.; Duyne, R. P. V. *J. Phys. Chem. B* **2000**, *104*, 10549.
(8) Jensen, T. R.; Kelly, L.; Lazarides, A.; Schatz, G. C. *J. Cluster Sci.* **1999**, *10*, 295.
(9) Bulgarevich, D. S.; Futamata, M. *Appl. Spectrosc.* **2004**, *58*, 757.
(10) Stockle, R. M.; Suh, Y. D.; Deckert, V.; Zenobi, R. *Chem. Phys. Lett.* **2000**, *318*, 131.
(11) Anderson, M. S. *Appl. Phys. Lett.* **2000**, *76*, 3130.
(12) Hartschuh, A.; Sanchez, E. J.; Xie, X. S.; Novotny, L. *Phys. Rev. Lett.* **2003**, *90*, 095503.
(13) Anderson, N.; Hartschuh, A.; Cronin, S.; Novotny, L. *J. Am. Chem. Soc.* **2005**, *127*, 2533.
(14) Pettinger, B.; Ren, B.; Picardi, G.; Schuster, R.; Ertl, G. *Phys. Rev. Lett.* **2004**, *92*, 096101.
(15) Mie, G. *Ann. Phys.* **1908**, *25*, 377.
(16) Kelly, K. L.; Coronado, E.; Zhao, L. L.; Schatz, G. C. *J. Phys. Chem. B* **2003**, *107*, 668.
(17) Malinsky, M. D.; Kelly, K. L.; Schatz, G. C.; Duyne, R. P. V. *J. Phys. Chem. B* **2001**, *105*, 2343.
(18) Jensen, T. R.; Duval, M. L.; Kelly, L.; Lazarides, A.; Schatz, G. C.; Duyne, R. P. V. *J. Phys. Chem. B* **1999**, *103*, 9846.
(19) Kottmann, J. P.; Martin, O. J. F. *Opt. Express* **2000**, *6*, 213.
(20) Kottmann, J. P.; Martin, O. J. F.; Smith, D. R.; Schultz, S. *Chem. Phys. Lett.* **2001**, *341*, 1.
(21) Denk, W.; Pohl, D. W. *J. Vac. Sci. Technol. B* **1991**, *9*, 510.
(22) Novotny, L.; Bian, R. X.; Xie, X. S. *Phys. Rev. Lett.* **1997**, *79*, 645.
(23) Milner, R. G.; Richards, D. *J. Microsc.* **2001**, *2002*, 66.
(24) Festy, F.; Demming, A.; Richards, D. *Ultramicroscopy* **2004**, *100*, 437.
(25) Krug, J. T.; Sanchez, E. J.; Xie, S. X. *J. Chem. Phys.* **2002**, *116*, 10895.
(26) Micic, M.; Klymyshyn, N.; Suh, Y. D.; Lu, H. P. *J. Phys. Chem. B* **2003**, *107*, 1574.
(27) Martin, Y. C.; Hamann, H. F.; Wickramasinghe, H. K. *J. Appl. Phys.* **2001**, *89*, 5774.
(28) Lynch, D. W.; Hunter, W. R. In *Handbook of Optical Constants of Solids*; Palik, E. D., Ed.; Academic Press: New York, 1985; p 292.
(29) Linnert, T.; Mulvaney, P.; Henglein, A.; Weller, H. *J. Am. Chem. Soc.* **1990**, *112*, 4657.
(30) Hodak, H. J.; Martini, I.; Hartland, G. V. *J. Phys. Chem. B* **1998**, *102*, 6958.
(31) Roberti, T. W.; Smith, B. A.; Zhang, J. Z. *J. Chem. Phys.* **1995**, *102*, 3860.
(32) Compagnini, G.; Scalisi, A. A.; Puglisis, O. *Phys. Chem. Chem. Phys.* **2002**, *4*, 2787.
(33) Bohren, C. F.; Huffman, D. R. *Absorption and Scattering of Light by Small Particles*; John Wiley & Sons: New York, 1983.
(34) Ren, B.; Picardi, G.; Pettinger, B. *Rev. Sci. Instrum.* **2004**, *75*, 837.
(35) Libioulle, L.; Houbion, Y.; Gilles, J.-M. *J. Vac. Sci. Technol. B* **1995**, *13*, 1325.
(36) Sick, B.; Hecht, B.; Novotny, L. *Phys. Rev. Lett.* **2000**, *85*, 4482.
(37) Gozhenko, V. V.; Grechko, L. G.; Whites, K. W. *Phys. Rev. B* **2003**, *68*, 125422.
(38) *Surface Plasmons*; Raether, H., Ed.; Springer: Berlin, 1988; Vol. 111.
(39) Mochizuki, S.; Ruppin, R. *J. Phys.: Condens. Matter* **1991**, *3*, 10037.